

Proceedings of the Fifth International Conference on  
Railway Technology:  
Research, Development and Maintenance  
Edited by J. Pombo  
Civil-Comp Conferences, Volume 1, Paper 18.3  
Civil-Comp Press, Edinburgh, United Kingdom, 2022, doi: 10.4203/ccc.1.18.3  
©Civil-Comp Ltd, Edinburgh, UK, 2022

## **Parameter optimization with respect to elongated hillock regions beside the high-speed railway under crosswinds**

**Zheng-Wei Chen<sup>1,2</sup> and Yi-Qing Ni<sup>1,2</sup>**

**<sup>1</sup>National Rail Transit Electrification and Automation  
Engineering Technology Research Center (Hong Kong Branch),  
Hung Hom, Kowloon, Hong Kong SAR, China**

**<sup>2</sup>Department of Civil and Environmental Engineering, The Hong  
Kong Polytechnic University, Hung Hom, Kowloon, Hong Kong  
SAR, China**

### **Abstract**

Complex terrains will result in elongated hillocks occurring near the windbreak wall along high-speed railways, furthermore, the hillock weakens the anti-wind ability of the windbreak wall. In this paper, characteristic parameters - the distance between hillock and windbreak wall ( $D$ ) and the hillock height ( $H$ ) are optimized by capitalizing on computational fluid dynamics (CFD) and multi-objective optimization method of the Non-dominated Sorting Genetic Algorithm II (NSGA-II). The surrogate model of Kriging model is advantaged and it is to be the final surrogate model to optimize the maximum wind speed  $U_{\max}$  and peak-to-peak value  $U_{p-p}$  for the railway concerned. The optimized results demonstrate that  $D = 25 - 35$  m and  $H = 2 - 12$  m can ensure that  $U_{\max} < 0.5$ . Besides, it is shown that distance  $D$  plays a key role in reducing the sudden wind peak values.

**Keywords:** windbreak wall, crosswind, high-speed railway, NSGA-II.

### **1 Introduction**

The effect of strong winds on trains is an intractable problem all over the world and attracts many researchers' attention [1, 2]. In China, part of the railway passes through the strong wind area, and diverse windproof facilities are constructed to mitigate the

wind impact [3], including the vertical plate-type windbreak wall, open-hole anti-wind tunnel, and porous windbreak wall, etc. Owing to complicated terrains along the railway, different transition regions generated beside the railway and impair the anti-wind property of windproof facilities. The effect of these transition regions has been studied in detail by Sun et al.[4]

Generally, Unified and continuous windbreak walls with a height of 3.5 m or 4 m provide the capability of ensuring the safe operation for the high-speed train. However, the full-scale test found that the train had a remarkable yawing phenomenon in some regions with uniform 3.5 m high windbreak wall. After conducting on-site investigations and comparing the time-history aerodynamic forces combined with the railway mileages, it indicated that some elongated hillocks near the windbreak occurred. The height of such hillocks is equivalent to or higher than the height of the windbreak wall. Thereby, the windproof ability of the windbreak wall is weakened greatly [5].

To account for the effect of elongated hillocks, this paper optimizes the flow structures and obtains a rational range of the height ( $H$ ) of hillock and the distance ( $D$ ) from the windbreak wall. The optimization targets are the maximum value and peak-to-peak value of the wind speed coefficient ( $U_{max}$  and  $U_{p-p}$ ) in the center of railway. The wind speed coefficient is defined as the ratio between the wind speed in the railway and the wind speed outside the windbreak wall. As shown in Figure 1, by considering real conditions, the optimal range of  $D$  is 0 – 60 m and the optimal range of  $H$  is 2 – 12 m.

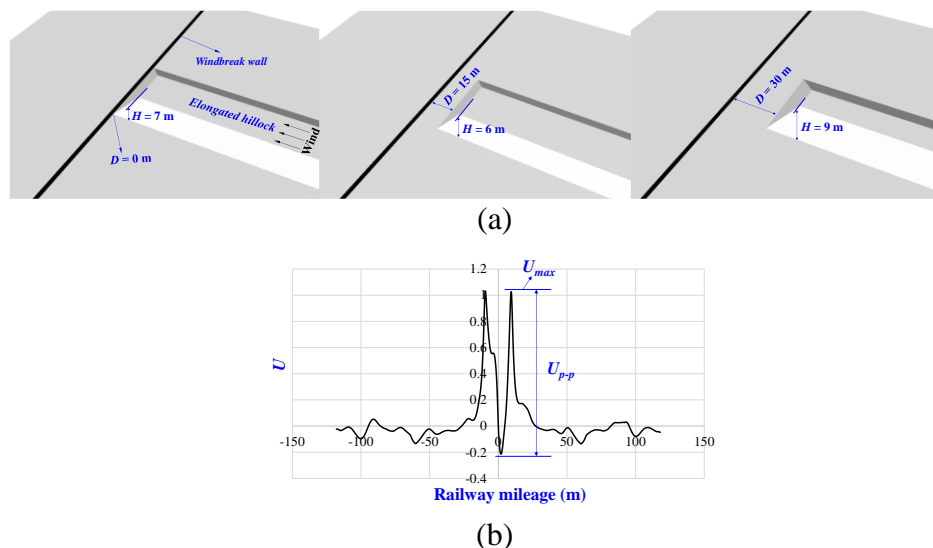


Figure 1: The optimization parameters and targets: (a) the distance  $D$  and hillock height  $H$ , (b) the optimization targets  $U_{max}$  and  $U_{p-p}$ .

## 2 Methods

The optimization method utilized in this paper is the Non-dominated Sorting Genetic Algorithm II (NSGA-II), and the sample points are picked out by the optimal Latin

hypercube (OLH) design method. The total 13 samples are calculated by the computational fluid dynamics (CFD) method.

Based on the commercial CFD code Fluent, the improved delayed detached eddy simulation (IDDES) method with SST  $k-\omega$  turbulence model is chosen to analyse the wind field and the distribution of  $U_{max}$  and  $U_{p-p}$ . The traditional detached eddy simulation (DES) method potentially produces modeled-stress depletion (MSD), which in some situations can lead to early separation, namely the grid-induced separation (GIS) effect. This effect is related to the grid spacing rather than to the physical properties of turbulence. The IDDES is a hybrid method combining the delayed detached eddy simulation (DDES) and wall-modeled large eddy simulation (WMLES), offers advantages for overcoming MSD and GIS, and for reducing the limitation of the Reynolds number for near-wall flow. The IDDES method has achieved enormous success in the field of train aerodynamics and flow analysis [6]. In addition, the surrogate model should be established to carry out the optimization process by NSGA-II. The algorithm of NSGA-II can reduce the computational complexity while ensuring the diversity of the population, and it is accompanied by a high optimization efficiency [7]. Disparate surrogate models are compared in this work, such as the response surface model (RSM), radial basis function neural network (RBFNN), and Kriging model. The detailed optimization process can refer to Chen and Ni [8].

### 3 Results

The coefficient of determination,  $R^2$ , of different surrogate models is tabulated in Table 1.  $R^2$  of the Kriging model for  $U_{max}$  and  $U_{p-p}$  is 0.895 and 0.936, respectively. Therefore, the Kriging model is chosen as the surrogate model to implement the optimization process by the NSGA-II method. Furthermore, the relationship between design variables and optimization goals are demonstrated in Figure 2. Comparing the effect of parameter variables  $D$  and  $H$ , it can be found that the influence of  $D$  is greater.

The relationship between  $U_{max}$  and  $U_{p-p}$  is depicted in Figure 3(a), due to backflows are not strong, the  $U_{p-p}$  is larger than  $U_{max}$  slightly. As shown in Figure 3(b), in the situation where  $U_{max} < 0.5$ , the corresponding  $D$  and  $H$  are 25 – 35 m and 2 – 12 m, respectively. Also, as long as the hillock is far enough from the windbreak wall, the effect of hillock height can be negligible. To verify the reliability of optimized and predicting results, extra three cases are computed by CFD. As illustrated in Figure 4 and Table 2, the error (defined in Equation (1)) for  $U_{max}$  is less than 8%, and the discrepancy for  $U_{p-p}$  is less than 5%. The deviation of  $U_{max}$  is larger on account of the small base value. Overall, the optimized and prediction results are in good agreement with the CFD results, which can be taken as a reference to guide actual construction.

Target parameters	RSM	RBFNN	Kriging
$U_{max}$	0.758	0.857	0.895
$U_{p-p}$	0.565	0.643	0.936

Table 1: The coefficient of determination,  $R^2$ , of different surrogate models.

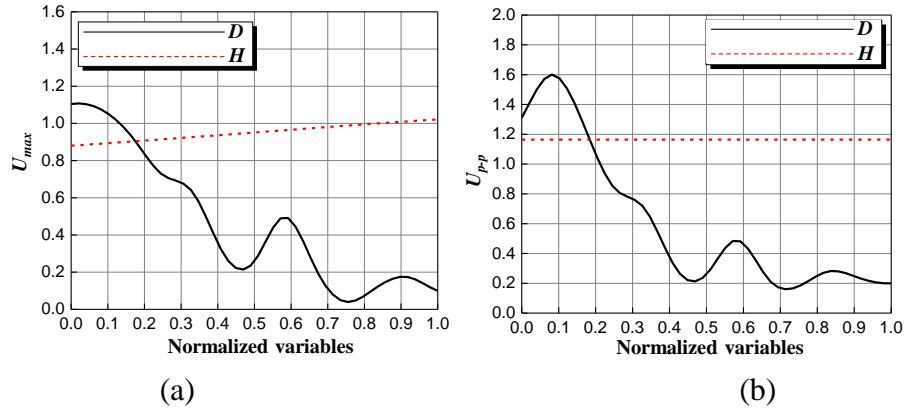


Figure 2: The relationship between the optimization parameters and targets: (a)  $U_{max}$ , (b)  $U_{p-p}$ .

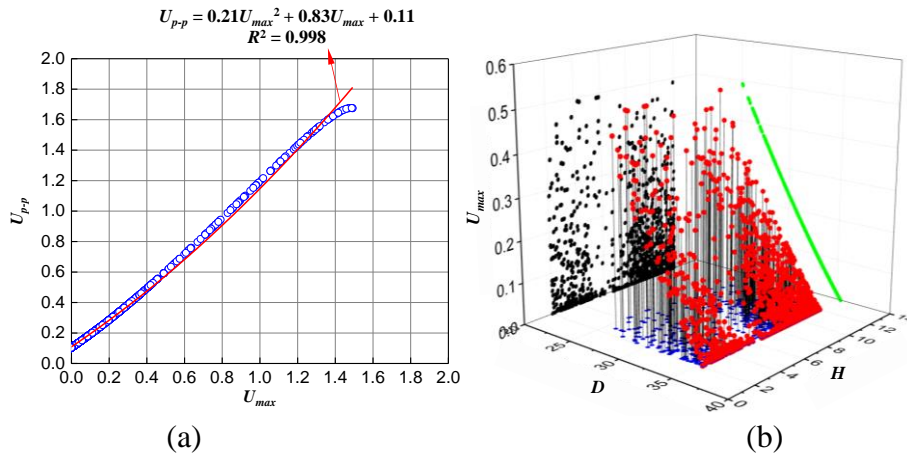


Figure 3: (a) The relationship between  $U_{max}$  and  $U_{p-p}$ , (b) the range of  $D$  and  $H$  when  $U_{max} < 0.5$ .

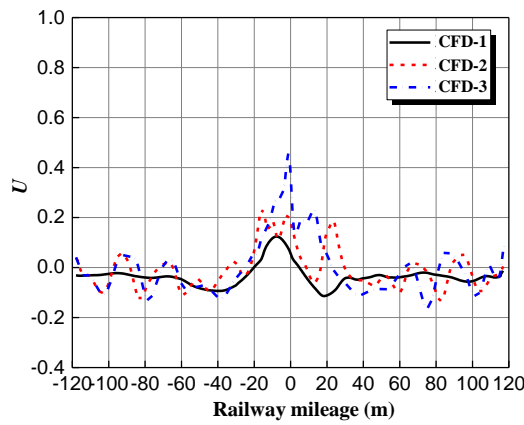


Figure 4: Three test cases of CFD results.

$$Error = \left| \frac{U_{prediction} - U_{CFD}}{U_{CFD}} \right| \quad (1)$$

No.	$D$ (m)	$H$ (m)	$U_{max}$			$U_{p-p}$		
			Prediction	CFD	Error	Prediction	CFD	Error
1	32.81	3.88	0.105	0.112	6.25%	0.196	0.205	4.39%
2	29.78	9.71	0.237	0.221	7.24%	0.332	0.317	4.73%
3	24.67	5.67	0.513	0.486	5.56%	0.618	0.598	3.34%

Table 2: Comparison between the prediction and CFD results.

## 4 Conclusions and Contributions

Employing the computational fluid dynamics (CFD) and the Non-dominated Sorting Genetic Algorithm II (NSGA-II), this study figured out the parameter optimization of a characteristic elongated hillock region beside a railway.

By adopting the optimal Latin hypercube design, 13 sample points are obtained to conduct the CFD simulation. Among three surrogate models, the Kriging model shows a good representation ability on the wind speed coefficient of  $U_{max}$  and  $U_{p-p}$  in the railway.

The research results indicate that the distance ( $D$ ) from the hillock to the windbreak wall is a critical variable, and the hillock height  $H$  is a minor factor. In cases studied in this paper, to meet the peak value of wind speed coefficient  $U_{max} < 0.5$ , the corresponding optimized parameters  $D = 25 - 35$  m and  $H = 2 - 12$  m are recommended

## Acknowledgements

The work described in this paper was supported by a grant (RIF) from the Research Grants Council of the Hong Kong Special Administrative Region (SAR), China (Grant No. R-5020-18) and a grant from the National Natural Science Foundation of China (Grant No. U1934209). The authors would also like to appreciate the funding support by the Innovation and Technology Commission of the Hong Kong SAR Government (Grant No. K-BBY1), The Hong Kong Polytechnic University's Postdoc Matching Fund Scheme (Grant No. 1-W16W), and the Open Project of Key Laboratory of Traffic Safety on Track of Ministry of Education, Central South University (Grant No. 502401002).

## References

- [1] Z.W. Chen, T.H. Liu, M. Li, M. Yu, Z.J. Lu, D.R. Liu, "Dynamic response of railway vehicles under unsteady aerodynamic forces caused by local landforms", *Wind and Structures*, 29(3): 149-161, 2019.
- [2] H. Hemida, S. Krajnović, "LES study of the influence of a train-nose shape on the flow structures under cross-wind conditions", *Journal of Fluids Engineering*, 130(9), 091101, 2008.
- [3] H.Q. Tian, "Review of research on high-speed railway aerodynamics in China", *Transportation Safety and Environment*, 1(1), 1-21, 2019.
- [4] Z. Sun, S.A. Hashmi, H. Dai, X. Cheng, T. Zhang, Z.W. Chen, "Safety comparisons of a high-speed train's head and tail passing by a windbreak breach", *Vehicle system dynamics*, 59(6), 823-840, 2021.

- [5] Z.W. Chen, T.H. Liu, M. Yu, G. Chen, M. Chen, Z.J. Guo, "Experimental and numerical research on wind characteristics affected by actual mountain ridges and windbreaks: a case study of the Lanzhou-Xinjiang high-speed railway", *Engineering Applications of Computational Fluid Mechanics*, 14(1), 1385-1403, 2020.
- [6] X.S. Huo, T.H. Liu, Z.W. Chen, W.H. Li, H.R. Gao, "Effect of the formation type with different freight vehicles on the train aerodynamic performance", *Vehicle System Dynamics*, 1, 1-29, 2021.
- [7] K. Deb, A. Pratap, S. Agarwal, T.A.M. Meyarivan, "A fast and elitist multiobjective genetic algorithm: NSGA-II", *IEEE transactions on evolutionary computation*, 6(2), 182-197, 2002.
- [8] Z.W. Chen, Y.Q. Ni, "Multi-objective optimization of the transition region of windbreak walls beside a railway", in *3rd International Conference on Industrial Aerodynamics*, Changchun, 2019.